



QUANTUM TRANSPORT AND OPTOELECTRONICS

Pablo Jarillo-Herrero
MASSACHUSETTS INSTITUTE OF TECHNOLOGY

11/30/2016
Final Report

DISTRIBUTION A: Distribution approved for public release.

Air Force Research Laboratory
AF Office Of Scientific Research (AFOSR)/ RTB1
Arlington, Virginia 22203
Air Force Materiel Command

REPORT DOCUMENTATION PAGE				Form Approved OMB No. 0704-0188	
<p>The public reporting burden for this collection of information is estimated to average 1 hour per response, including the time for reviewing instructions, searching existing data sources, gathering and maintaining the data needed, and completing and reviewing the collection of information. Send comments regarding this burden estimate or any other aspect of this collection of information, including suggestions for reducing the burden, to Department of Defense, Executive Services, Directorate (0704-0188). Respondents should be aware that notwithstanding any other provision of law, no person shall be subject to any penalty for failing to comply with a collection of information if it does not display a currently valid OMB control number.</p> <p>PLEASE DO NOT RETURN YOUR FORM TO THE ABOVE ORGANIZATION.</p>					
1. REPORT DATE (DD-MM-YYYY) 30-11-2016		2. REPORT TYPE Final Performance		3. DATES COVERED (From - To) 01 Aug 2011 to 31 Jul 2016	
4. TITLE AND SUBTITLE QUANTUM TRANSPORT AND OPTOELECTRONICS IN GAPPED GRAPHENE NANODEVICES				5a. CONTRACT NUMBER	
				5b. GRANT NUMBER FA9550-11-1-0225	
				5c. PROGRAM ELEMENT NUMBER 61102F	
6. AUTHOR(S) Pablo Jarillo-Herrero				5d. PROJECT NUMBER	
				5e. TASK NUMBER	
				5f. WORK UNIT NUMBER	
7. PERFORMING ORGANIZATION NAME(S) AND ADDRESS(ES) MASSACHUSETTS INSTITUTE OF TECHNOLOGY 77 MASSACHUSETTS AVE CAMBRIDGE, MA 02139-4301 US				8. PERFORMING ORGANIZATION REPORT NUMBER	
9. SPONSORING/MONITORING AGENCY NAME(S) AND ADDRESS(ES) AF Office of Scientific Research 875 N. Randolph St. Room 3112 Arlington, VA 22203				10. SPONSOR/MONITOR'S ACRONYM(S) AFRL/AFOSR RTB1	
				11. SPONSOR/MONITOR'S REPORT NUMBER(S) AFRL-AFOSR-VA-TR-2016-0358	
12. DISTRIBUTION/AVAILABILITY STATEMENT A DISTRIBUTION UNLIMITED: PB Public Release					
13. SUPPLEMENTARY NOTES					
14. ABSTRACT <p>The research objective of this proposal is to investigate the quantum electronic and optoelectronic properties of graphene-based semiconducting nanodevices. To achieve this we will combine optoelectronic and plasmonic device structures with atomically seamless electrical contacts. The devices will be based on fully band gap engineered bilayer graphene and graphene nanoribbons, resulting in all-carbon nanoelectronic devices with optoelectronic properties and functionalities (such as temporally and spatially tunable band gap energies) not possible with conventional materials. Importantly, this device technology will be developed using hexagonal boron nitride as a dielectric, which has been demonstrated to vastly improve the electronic properties of substrate-supported graphene and is already under investigation in the Jarillo-Herrero group. The electronic device structures described in this proposal will demonstrate the powerful role graphene can play in practical high-technology applications since we will be directly measuring high-speed Zener diodes and PN junctions, as well as FET and band-engineered 1D tunneling transistors. These device structures may operate at unprecedented speeds and with tremendous efficiency, both of which are vital for aeronautic and defense technologies.</p>					
15. SUBJECT TERMS quantum transport, nanodevices, graphene					
16. SECURITY CLASSIFICATION OF:			17. LIMITATION OF ABSTRACT UU	18. NUMBER OF PAGES	19a. NAME OF RESPONSIBLE PERSON WEINSTOCK, HAROLD
a. REPORT Unclassified	b. ABSTRACT Unclassified	c. THIS PAGE Unclassified			

Standard Form 298 (Rev. 8/98)
Prescribed by ANSI Std. Z39.18

DISTRIBUTION A: Distribution approved for public release.

				19b. TELEPHONE NUMBER <i>(Include area code)</i> 703-696-8572
--	--	--	--	---

Contract/Grant Title: Quantum Transport and Optoelectronics in Gapped Graphene Nanodevices

Contract/Grant #: FA9550-11-1-0225

Final Report

During the period funded by this grant, we investigated the fundamental physical processes of light-matter interactions in van der Waals crystals, including graphene, boron nitride, transition metal dichalcogenides and heterostructures formed from them. Our research leads to deep understanding of novel physics embedded in the low dimensionality, such as ultrafast electron-electron interaction, unconventional electron-phonon coupling and strong light confinement. This understanding paves the way for creating high-performance optoelectronic and energy harvesting devices with state-of-the-art functionalities, equipped by these innovative materials and unique device architectures. This grant has resulted in 12 high profile publications, including two papers in *Science*[1, 2], two in *Nature Physics*[3, 4], two in *Nature Nanotechnology*[5, 6], two in *Nature Communications*[7, 8], one in *Physical Review Letters*[9], two in *Nano Letters*[10, 11] and one in *Advance Materials*[12]. Below we highlight a few major works funded by AFOSR.

1. Hot Carrier-Assisted Photoresponse in Intrinsic Graphene[1, 6, 9]

The photoresponse of materials, which determines the performance of optoelectronic devices, is governed by energy relaxation pathways of photoexcited electron-hole pairs: energy transferred to the lattice is lost as heat, while energy retained in the electronic subsystem can be used to drive an optoelectronic circuit. In graphene, energy relaxation pathways are strongly affected by a vanishing electronic density of states, which creates a bottleneck that limits energy transfer into the lattice. As a result, the photogenerated carrier population remains hot while the lattice stays cool.

In graphene, hot carriers should play a key role in the optoelectronic response. Initial studies observed photocurrent response both at graphene-metal contacts and monolayer-bilayer graphene junctions, yet the underlying mechanism was under debate between the photovoltaic (PV) effect, where the photogenerated electron-hole pairs are separated by a built-in electric field [13-15], and the photothermoelectric (PTE) effect, driven by electron temperature gradients [16]. In our work, we carried out scanning photocurrent measurements of highly controllable dual-gated graphene p-n junction devices (Fig. 3a) to resolve this debate. Tuning the bottom- and top-gate voltages, V_{BG} and V_{TG} respectively, allowed independent control of carrier density of electrons and holes in each region to form a p-n junction interface at the middle of the device (Fig. 3b) [17-19]. Figure 3d shows a photocurrent image obtained by scanning a focused (1 μm) laser spot over the device (Fig. 3c) while measuring the current I .

Our measurements indicated that hot electronic carriers dominate the intrinsic optoelectronic response of graphene in the linear optical power regime. The hot carrier regime manifests as a strong PTE effect that results in a striking six-fold sign-alternating photocurrent pattern as a function of gate voltages (Fig. 3e), qualitatively different from the PV effect which would only

have a two-fold sign-alternating photocurrent pattern. Additionally, the spatial pattern and the charge density dependence of the photoresponse established a strong connection between thermal energy transport and electronic charge transport. In line with this finding, the graphene p-n junction device can be operated as a novel photo-thermometer that measures local electron temperature. In collaboration with the Koppens group in ICFO, we carried out a time-resolved photovoltage measurement and resolved a voltage generation time of less than 50 femtoseconds. This ultrafast response was further demonstrated by electrically measuring the pulse duration of a sub-50 femtosecond laser pulse. The above results have been published in *Science* [1] and *Nature Nanotechnology* [6].

Continuing this line of work, we performed a systematic temperature dependence of the PTE current to determine the dominant hot carrier cooling channels in graphene. A persisting six-fold pattern at all temperatures (4 – 300 K) indicates that the PTE effect always governs the photocurrent response, allowing us to track the induced electron temperature and probe hot electron cooling mechanisms. We observed a pronounced non-monotonic temperature dependence of the PTE photocurrent (Fig. 3f), which we understand as the competition between two hot electron cooling pathways, i.e., momentum-conserving normal collisions that dominate at low temperatures and disorder-assisted supercollisions that dominate at high temperatures [20–22]. The peak temperature, where the total cooling rate is minimal, strongly depends on charge carrier density and disorder strength, thus allowing for an unprecedented way of controlling graphene's photoresponse. This work was selected as an *Editors' Suggestion* in *Physical Review Letters* [9].

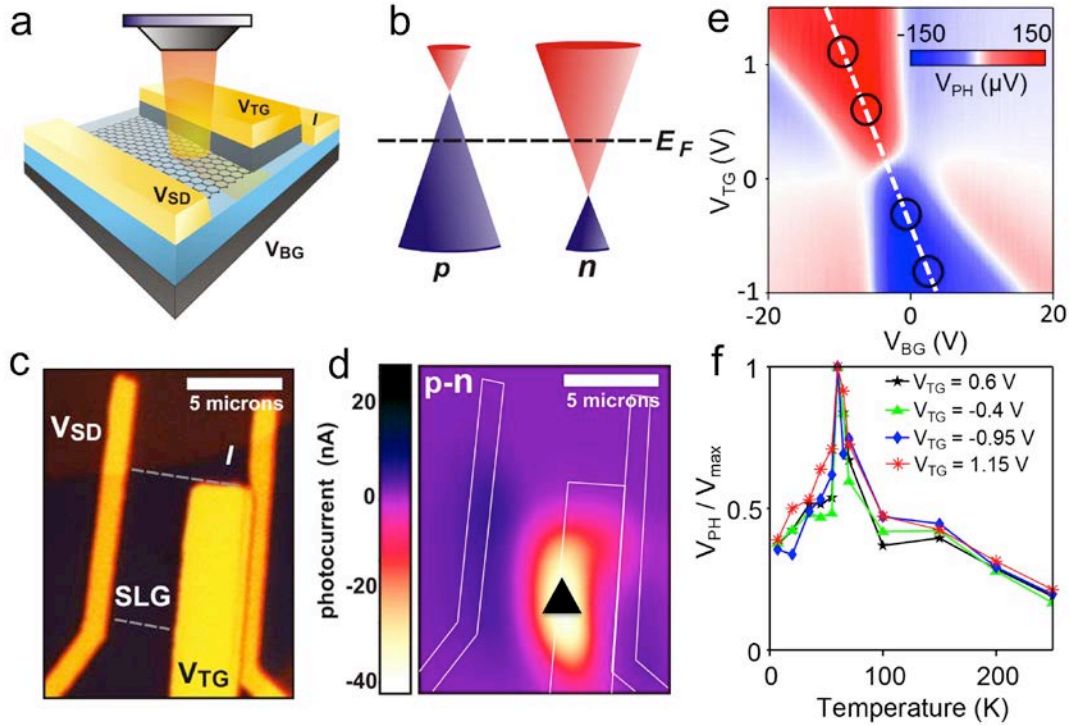


Figure 1. Hot carrier-assisted photoresponse in graphene and its dependence on sample

temperatures. **a**, Photocurrent measurement scheme with scanning laser excitation. **b**, Schematic of band alignment for a monolayer graphene p-n junction. **c**, Optical micrograph of a dual-gated graphene device incorporating BN as the top gate dielectric. **d**, Spatially resolved photocurrent map with laser wavelength 850 nm. White lines mark the location of gold contacts and top gate electrode. **e**, Photocurrent of the graphene p-n junction versus back-gate and top-gate voltages, measured with the laser fixed at the p-n interface (black triangle in **d**). The six-fold pattern of the photovoltage sign changes provides evidence that the PTE effect rather than the PV effect dominates the intrinsic photoresponse in graphene. **f**, The photovoltage as a function of the sample temperature (normalized to the maximum value) at particular gate voltage values (black circles in **e**) along the white dashed line, where the chemical potentials are equal but opposite in signs at the two parts.

2. Tuning Electron Thermalization Pathways in a van der Waals Heterostructure[3]

Immediately after photoexcitation of an optoelectronic device, energetic electrons scatter with other high-energy and ambient charge carriers to form a thermalized hot electron gas, which further cools by dissipating excess energy to the lattice. Due to the short distance travelled by charge carriers between electron-electron scattering events in solids [23], equilibration among the electrons occurs on the tens of femtoseconds to picosecond time scales [24, 25]. In graphene, a low-dimensional material with much enhanced Coulomb interaction[26], electron thermalization is known to occur on extremely fast time scales (<30 fs) [6, 27-29], reflecting the extremely short transit length between scattering events. Most analyses of graphene have, therefore, treated its electrons to be instantaneously thermalized [1, 9, 20, 21], and slightly non-thermal electronic behavior has thus far only been reported in pump-probe experiments with ultrashort (~ 10 fs) laser pulses and low excitation density [30, 31]. Due to such short time (femtosecond) and length (nanometer) scales, it is challenging to detect and control the thermalization process in graphene, or more generally, in any solid-state systems.

We take a novel approach to probe and manipulate electron thermalization in graphene by introducing a new energy transport channel that competes with the thermalization process. Such an additional dynamical pathway is realized in a van der Waals heterostructure that consists of a graphene-BN-graphene stack (Fig. 4a-c). In this layered structure, the photoexcited electrons in one graphene layer can travel vertically to the other graphene layer through the very thin middle BN layer (blue dashed arrow in Fig. 4b). Given the close proximity of these layers, *interlayer* charge transport can occur on extremely fast time scales, competing directly with the *intralayer* thermalization process (red arrows in Fig. 4b).

In our experiment, we have observed such a competition by measuring the interlayer photocurrent under different bias and excitation conditions (color map shown in Fig. 4d-e). In particular, we observe distinct power-dependences of the photocurrent in the different regimes, as shown in Fig. 4f. Region A (low photon energy and low bias voltage) shows highly-superlinear power dependence, whereas Region B (high photon energy and high bias voltage) shows linear power dependence. These two distinct power dependences are attributed to two distinct photocurrent generation mechanisms in our structure: thermionic emission and direct tunneling. By adjusting the interlayer bias voltage and/or the excitation photon energy, we can

tune the *interlayer* charge transport to be slower or faster than the *intralayer* thermalization, thus tuning the overall thermalization process.

Our experiments not only provide valuable insight into the electron dynamics of graphene, but also demonstrate a new means to manipulate electron thermalization in low-dimensional materials. With appropriate modeling, we have deduced the thermalization time in graphene (~ 10 fs) from a time-averaged transport experiment (Fig. 4f black dashed lines). Similar experimental methods can readily be extended to other van der Waals heterostructures to probe their ultrafast electronic processes. More generally, given the central role that electron thermalization plays in energy transport, the tunability on femtosecond time scales demonstrated in our research opens up a new range of in-situ functionality for novel optoelectronic devices. This work was recently published in *Nature Physics*[3].

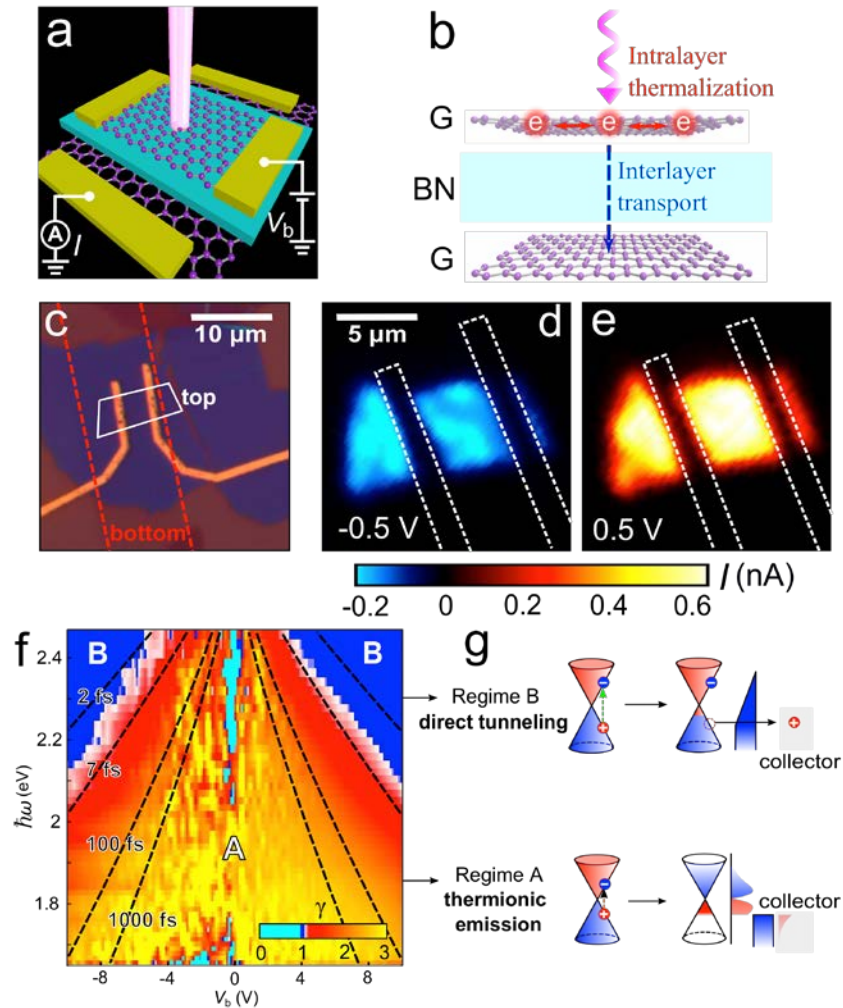


Figure 2. Interlayer photocurrent of a G-BN-G device. **a**, Schematic of a G-BN-G device under optical excitation. **b**, Schematic of *intralayer* thermalization and *interlayer* transport of the optically excited carriers. **c**, Optical image of a G-BN-G device, which consists of a top exfoliated graphene layer (white line), a 14-nm-thick BN flake, and a bottom graphene layer grown by chemical vapor deposition (dashed red line). **d-e**, Scanning images of interlayer

photocurrent at interlayer bias $V_b = -0.5$ and 0.5 V. **f**, A color map of γ , the exponent of the power-dependence of the photocurrent, as a function of V_b and $\hbar\omega$. The color scale is customized to make the area with $\gamma > 1$ (Region A) and $\gamma = 1 \pm 0.02$ (Region B) appear red-yellow and blue, respectively. The black dashed lines are theoretical contours corresponding to tunneling time of 2, 7, 100 and 1000 fs, predicted by our model described in Ref. [3]. **g**, Schematics depicting the thermionic emission and the direct carrier tunneling as the dominant photocurrent mechanism for Region A and B in (f), respectively. All measurements were carried out with a supercontinuum laser at $T = 100$ K.

3. Collective Excitations in Hexagonal Boron Nitride and Graphene[2, 5, 7]

Hexagonal boron nitride has been widely used as high quality substrate for low-dimensional materials and also as a capping layer to protect these materials from atmospheric contaminants and oxidation[32, 33]. In addition, heterostructures of BN with other 2D materials can form superlattices (or moiré patterns), which strongly alter the combined electronic properties[34-36]. As a polar material, light can strongly couple to BN’s optical phonon resonance, and the layered nature can lead to novel properties of this resonance. We collaborated with Prof. Dimitri Basov’s group at UC San Diego to investigate phonon-polariton propagation in this layered material using an infrared nanoimaging technique in a scattering-type near field scanning optical microscope (s-SNOM).

We launched, detected, and imaged polaritonic waves in real space and altered their wavelength by varying the number of crystal layers (Fig. 5a-g). The measured dispersion of polaritonic waves was shown to be governed by the crystal thickness according to a scaling law that persists down to a few atomic layers. We also discovered that, at certain frequencies, BN exhibits hyperbolic properties: the axial and tangential permittivities have opposite signs. In such circumstances light propagation is unusual, leading to novel optical phenomena. We reported infrared nano-imaging experiments demonstrating that BN can act as a “hyper-focusing lens” and as a multi-mode waveguide in mid-infrared frequencies. The lensing is manifested by subdiffractional focusing of phonon-polaritons launched by pre-made metallic patterns underneath the BN crystal (Fig. 5h-i). Our work opens new opportunities for anisotropic layered insulators in infrared nanophotonics complementing and potentially surpassing concurrent artificial hyperbolic materials with lower losses and higher optical localization. This work was published in *Science* [2] and *Nature Communications* [7].

In addition, we have implemented and investigated the tunable hyperbolic response in heterostructures comprised of a monolayer graphene deposited on hexagonal boron nitride (G-BN) slabs. Electrostatic gating of the graphene layer enables electronic tuning of the phonon-polariton properties in BN. The tunability originates from the hybridization of surface plasmon-polaritons in graphene to hyperbolic phonon-polaritons in BN, which we examined via nano-IR imaging and spectroscopy. These hybrid polaritons possess a combination of properties from plasmons in graphene and phonon-polaritons in BN. Therefore, G-BN structures fulfill the definition of an electromagnetic metamaterial, since the combined properties of these devices is

not revealed by the constituent elements alone. Our results uncover a practical approach for realization of nano-photonic metamaterials by exploiting the interaction of distinct types of polaritonic modes hosted by different constituent layers in van der Waals heterostructures. This work was published in *Nature Nanotechnology* [5].

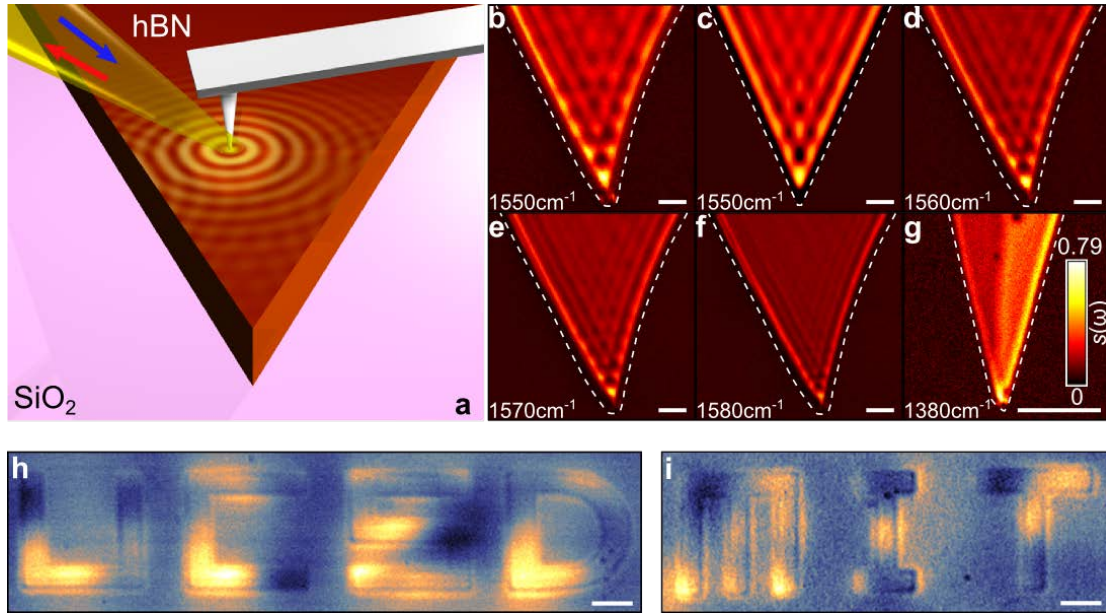


Figure 3. Real-space imaging of surface phonon-polaritons on BN and a BN-based ‘hyperlens’. **a**, Schematics. Arrows denote the incident and back-scattered IR light. Concentric yellow circles illustrate the phonon polariton waves launched by the AFM tip and reflected by the two edges of a tapered BN crystal. **(b and d to f)** IR near-field images of the normalized amplitude signal and taken at different IR frequencies (BN thickness in **b** to **f** $d = 256$ nm). **c**, Simulation of the phonon-polariton interference pattern. **g**, Phonon-polaritons probed in three-layer (left) and four-layer (right) BN crystals. The white dashed line tracks the BN edges according to the AFM topography. Scale bars indicate 800 nm. **h-i**, Use BN as a hyper-lensing material to image the sub-diffractional structure (letter ‘UCSD’ and ‘MIT’) underneath.

References:

- [1] Gabor, N.M., et al., *Science* **334**, 648-652 (2011).
- [2] Dai, S., et al., *Science* **343**, 1125-1129 (2014).
- [3] Ma, Q., et al., *Nature Physics*, doi:10.1038/nphys3620 (2016).
- [4] Tielrooij, K., et al., *Nature Physics* **11**, 281-287 (2015).
- [5] Dai, S., et al., *Nature Nanotechnology* **10**, 682-686 (2015).
- [6] Tielrooij, K.-J., et al., *Nature Nanotechnology* **10**, 437-443 (2015).

- [7] Dai, S., et al., Nature Communications **6** 6963 (2015).
- [8] Woessner, A., et al., Nature Communications **7**, 10783 (2016).
- [9] Ma, Q., et al., Physical Review Letters **112**, 247401 (2014).
- [10] Hsu, A.L., et al., Nano Letters **15**, 7211-7216 (2015).
- [11] Herring, P.K., et al., Nano Letters **14**, 901-907 (2014).
- [12] Ling, X., et al., arXiv preprint arXiv:1512.04492, (2015).
- [13] Lee, E.J., et al., Nature Nanotechnology **3**, 486-490 (2008).
- [14] Park, J., et al., Nano Letters **9**, 1742-1746 (2009).
- [15] Xia, F., et al., Nature Nanotechnology **4**, 839-843 (2009).
- [16] Xu, X., et al., Nano Letters **10**, 562-566 (2009).
- [17] Özyilmaz, B., et al., Physical Review Letters **99**, 166804 (2007).
- [18] Lemme, M.C., et al., Nano Letters **11**, 4134-4137 (2011).
- [19] Williams, J., et al., Science **317**, 638-641 (2007).
- [20] Song, J.C., et al., Physical review letters **109**, 106602 (2012).
- [21] Graham, M.W., et al., Nature Physics **9**, 103-108 (2013).
- [22] Betz, A., et al., Nature Physics **9**, 109-112 (2013).
- [23] Kittel, C., et al., *Introduction to solid state physics*. Vol. 8. 1976: Wiley New York.
- [24] Lisowski, M., et al., Applied Physics A **78**, 165-176 (2004).
- [25] Fann, W., et al., Physical Review B **46**, 13592 (1992).
- [26] Neto, A.C., et al., Reviews of Modern Physics **81**, 109 (2009).
- [27] Tielrooij, K., et al., Nature Physics **9**, 248-252 (2013).
- [28] Brida, D., et al., Nature Communications **4**, 1987 (2013).
- [29] Song, J.C., et al., Physical Review B **87**, 155429 (2013).
- [30] Gierz, I., et al., Nature Materials **12**, 1119-1124 (2013).
- [31] Johannsen, J.C., et al., Physical Review Letters **111**, 027403 (2013).
- [32] Dean, C., et al., Nature Nanotechnology **5**, 722-726 (2010).
- [33] Wang, L., et al., Science **342**, 614-617 (2013).
- [34] Yankowitz, M., et al., Nature Physics **8**, 382-386 (2012).
- [35] Hunt, B., et al., Science **340**, 1427-1430 (2013).
- [36] Ni, G., et al., Nature Materials **14**, 1217-1222 (2015).

AFOSR Deliverables Submission Survey

Response ID:7164 Data

1.

Report Type

Final Report

Primary Contact Email

Contact email if there is a problem with the report.

pjarillo@mit.edu

Primary Contact Phone Number

Contact phone number if there is a problem with the report

6172533653

Organization / Institution name

MIT

Grant/Contract Title

The full title of the funded effort.

Quantum Transport and Optoelectronics in Gapped Graphene Nanodevices

Grant/Contract Number

AFOSR assigned control number. It must begin with "FA9550" or "F49620" or "FA2386".

FA9550-11-1-0225

Principal Investigator Name

The full name of the principal investigator on the grant or contract.

Pablo Jarillo-Herrero

Program Officer

The AFOSR Program Officer currently assigned to the award

Harold Weinstock

Reporting Period Start Date

07/31/2011

Reporting Period End Date

07/31/2016

Abstract

During the period funded by this grant, we investigated the fundamental physical processes of light-matter interactions in van der Waals crystals, including graphene, boron nitride, transition metal dichalcogenides and heterostructures formed from them. Our research has led to deep understanding of novel physics embedded in the low dimensionality, such as ultrafast electron-electron interaction, unconventional electron-phonon coupling and strong light confinement. This understanding paves the way for creating high-performance optoelectronic and energy harvesting devices with state-of-the-art functionalities, equipped by these innovative materials and unique device architectures. This grant has resulted in 12 high profile publications, including two papers in Science[1, 2], two in Nature Physics[3, 4], two in Nature Nanotechnology[5, 6], two in Nature Communications[7, 8], one in Physical Review Letters[9], two in Nano Letters[10, 11] and one in Advance Materials[12]. In the past year, we extended optoelectronic and hot carrier research in graphene to graphene based heterostructures, in combination with other two dimensional van der Waals materials, such as hexagonal boron nitride and transition metal dichalcogenides (MoS2, WSe2 etc.). These hybrid systems provide novel approaches to reveal intriguing properties of graphene hot carriers and build up versatile optoelectronic functionalities. In particular, we

DISTRIBUTION A: Distribution approved for public release.

realized controllable competing relaxation channels of photocarriers on time scales of ten femtoseconds, in a double graphene layer structure separated by 5-30 nanometers thick boron nitride. In this structure, by finely tuning the interlayer bias voltage or varying the excitation photon energy, the optically excited carriers can be precisely controlled to either relax primarily within the layer via electron-electron scattering or directly through interlayer transport. The energy conversion pathways can therefore be adjusted accordingly on ultrafast time scales.

Distribution Statement

This is block 12 on the SF298 form.

Distribution A - Approved for Public Release

Explanation for Distribution Statement

If this is not approved for public release, please provide a short explanation. E.g., contains proprietary information.

SF298 Form

Please attach your SF298 form. A blank SF298 can be found [here](#). Please do not password protect or secure the PDF. The maximum file size for an SF298 is 50MB.

[PJH+sf0298.pdf](#)

Upload the Report Document. File must be a PDF. Please do not password protect or secure the PDF. The maximum file size for the Report Document is 50MB.

[AFOSR+final+report.pdf](#)

Upload a Report Document, if any. The maximum file size for the Report Document is 50MB.

Archival Publications (published) during reporting period:

- [1] Gabor, N.M., et al., Science 334, 648-652 (2011).
- [2] Dai, S., et al., Science 343, 1125-1129 (2014).
- [3] Ma, Q., et al., Nature Physics 12, 455-459 (2016).
- [4] Tielrooij, K., et al., Nature Physics 11, 281-287 (2015).
- [5] Dai, S., et al., Nature Nanotechnology 10, 682-686 (2015).
- [6] Tielrooij, K.-J., et al., Nature Nanotechnology 10, 437-443 (2015).
- [7] Dai, S., et al., Nature Communications 6 6963 (2015).
- [8] Woessner, A., et al., Nature Communications 7, 10783 (2016).
- [9] Ma, Q., et al., Physical Review Letters 112, 247401 (2014).
- [10] Hsu, A.L., et al., Nano Letters 15, 7211-7216 (2015).
- [11] Herring, P.K., et al., Nano Letters 14, 901-907 (2014).
- [12] Ling, X., et al., Advanced Materials 28, 2322-2329 (2016).

New discoveries, inventions, or patent disclosures:

Do you have any discoveries, inventions, or patent disclosures to report for this period?

Yes

Please describe and include any notable dates

- Discovery of photothermal mechanism for photocurrent generation in graphene p-n junctions (2011) (no patent)
- Discovery of hot-carrier relaxation mechanisms in graphene (2014-16) (no patent)

Do you plan to pursue a claim for personal or organizational intellectual property?

No

Changes in research objectives (if any):

N/A

Change in AFOSR Program Officer, if any:

N/A

Extensions granted or milestones slipped, if any:

N/A

DISTRIBUTION A: Distribution approved for public release.

AFOSR LRIR Number

LRIR Title

Reporting Period

Laboratory Task Manager

Program Officer

Research Objectives

Technical Summary

Funding Summary by Cost Category (by FY, \$K)

	Starting FY	FY+1	FY+2
Salary			
Equipment/Facilities			
Supplies			
Total			

Report Document

Report Document - Text Analysis

Report Document - Text Analysis

Appendix Documents

2. Thank You

E-mail user

Oct 27, 2016 10:38:44 Success: Email Sent to: pjarillo@mit.edu